

Central exclusive production of scalar and pseudoscalar charmonia in the light-front k_T -factorization approach

Izabela Babiarz^{1,*}, Roman Pasechnik^{2,†}, Wolfgang Schäfer^{1,‡} and Antoni Szczurek^{1,3,§}

¹*Institute of Nuclear Physics, Polish Academy of Sciences,
ulica Radzikowskiego 152, PL-31-342 Kraków, Poland*

²*Department of Astronomy and Theoretical Physics, Lund University, SE-223 62 Lund, Sweden*

³*Faculty of Mathematics and Natural Sciences, University of Rzeszów,
ulica Pigońia 1, PL-35-310 Rzeszów, Poland*



(Received 19 August 2020; accepted 7 November 2020; published 18 December 2020)

We study exclusive production of scalar $\chi_{c0} \equiv \chi_c(0^{++})$ and pseudoscalar η_c charmonia states in proton-proton collisions at the LHC energies. The amplitudes for $gg \rightarrow \chi_{c0}$ as well as for $gg \rightarrow \eta_c$ mechanisms are derived in the k_T -factorization approach. The $pp \rightarrow pp\eta_c$ reaction is discussed for the first time. We have calculated rapidity, transverse momentum distributions, and such correlation observables as the distribution in relative azimuthal angle and (t_1, t_2) distributions. The latter two observables are very different for χ_{c0} and η_c cases. In contrast to the inclusive production of these mesons considered very recently in the literature, in the exclusive case, the cross section for η_c is much lower than that for χ_{c0} , which is due to a special interplay of the corresponding vertices and off-diagonal unintegrated gluon distributions used to calculate the cross sections. We present the numerical results for the key observables in the framework of potential models for the light-front quarkonia wave functions. We also discuss how different the absorptive corrections are for both considered cases.

DOI: [10.1103/PhysRevD.102.114028](https://doi.org/10.1103/PhysRevD.102.114028)

I. INTRODUCTION

The central exclusive diffractive processes in proton-proton collisions at high energies have attracted recently a lot of attention. These processes lead to very unusual final states. For example, in the central exclusive production, one produces one or a few particles at central rapidities which are fully measured. There are no other tracks in the detectors. The incoming protons remain intact (in the virtue of “elastic diffraction”) or are excited into small mass hadronic systems, which disappear into the beam pipe. We consider here simultaneously two such reactions, $pp \rightarrow p\chi_{c0}p$ and $pp \rightarrow p\eta_cp$, which are well suited to be analyzed in the framework of the so-called Durham model formulated by Khoze *et al.* (see Ref. [1] and references therein). From the experimental point of view, there is a rapidity gap, between each of the protons and the

produced χ_{c0} or η_c states. These processes hence provide a very clean environment for the study of the produced hadronic systems tightly connected to poorly known soft and semihard QCD dynamics. For a review of conceptual and experimental challenges with such central exclusive production (CEP) reactions, see for example Ref. [2].

The theory of the CEP of single χ_{cJ} , $J = 0, 1, 2$ mesons, with a correct account for the spin of the mesons and precise kinematics of the production process, has been worked out earlier by Pasechnik *et al.* (PST) in a series of papers [3–5]. The numerical calculations were done for the Tevatron energies. In this analysis, the nonrelativistic QCD (NRQCD) methods were applied. So far, only CEP of light pseudoscalar mesons was discussed in the literature [3,6]. There, rather nonperturbative effects strongly dominate (see Ref. [6]). Very recently, in Ref. [7], the production of χ_{c0} at the LHC was discussed in the k_T -factorization and saturation dipole-model inspired approaches. The analysis was performed there in the NRQCD approach and using a single model for the unintegrated gluon distribution (UGDs) and a particular prescription for the off-diagonal UGD. Given a particular importance of the CEP of heavy quarkonia for ongoing and future experimental studies, we revisit and extend this analysis to account for additional effects and sources for theoretical uncertainties (such as the shapes of the charmonia wave functions and a treatment of the absorptive corrections, as well as an accurate treatment

*izabela.babiarz@ifj.edu.pl

†roman.pasechnik@thep.lu.se

‡Wolfgang.Schafer@ifj.edu.pl

§antoni.szczurek@ifj.edu.pl

Published by the American Physical Society under the terms of the [Creative Commons Attribution 4.0 International license](https://creativecommons.org/licenses/by/4.0/). Further distribution of this work must maintain attribution to the author(s) and the published article's title, journal citation, and DOI. Funded by SCOAP³.

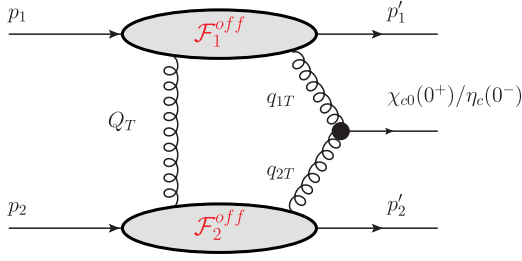


FIG. 1. Generic diagram for the Durham model approach to the considered exclusive production processes.

of the phase space and production kinematics) as well as incorporate the pseudoscalar η_c final state for the first time.

Recently, our group showed how to include relativistic corrections for the inclusive production of η_c [8] and χ_c [9]. These calculations use light-cone wave functions of charmonia which were derived from well known models for the $c\bar{c}$ interquark potential. It is the aim of the present paper to do a similar study for the exclusive case. In addition, there is no such a study on the $pp \rightarrow pp\eta_c$ CEP available in the literature. In contrast, inclusive production of $\eta_c(1S)$ was measured by the LHCb Collaboration in proton-proton collisions for $\sqrt{s} = 7, 8, 13$ TeV [10]. Is such a measurement possible for the exclusive production of η_c ? This study is a first step to address this important question. An analysis of inclusive diffractive production of $\eta_c(1S)$ was done recently in Ref. [11].

In the present paper, we wish to discuss in parallel the exclusive production process of both the scalar χ_{c0} and pseudoscalar η_c quarkonia. For illustration of the corresponding production mechanism initially proposed by the Durham group [1], see Fig. 1. We start with a brief introduction into the formalism for $pp \rightarrow p\chi_{c0}p$ and $pp \rightarrow p\eta_c p$ reactions based upon the Durham model of CEP [1] setting up the necessary notation and conventions. In this model, a quarkonium state is produced via fusion of two virtual active gluons accompanied by an extra exchange with a screening gluon as is shown in Fig. 1. The additional exchange of the gluon provides color conservation and hence the effective color singlet exchange in the t -channel. As a result, in the final state, in addition to the meson produced mainly at central rapidities, there are two forward protons that retain most of their initial energy. We intend to calculate the integrated cross sections for such processes as well as several differential distributions relevant for future measurements. We wish to discuss both the hard and soft processes involved in these reactions in the light-front QCD approach, to consider several prescriptions on how to calculate the off-diagonal UGDs (some of them have already been used previously in the literature) and to estimate the absorptive corrections in the differential distributions.

II. VIRTUAL GLUON FUSION INTO (PSEUDO)SCALAR CHARMONIA

Below, we shall consider the hard $\chi_{c0}(1P)$ and $\eta_c(1S)$ charmonia production subprocesses separately.

A. Light-cone amplitude for $g^*g^* \rightarrow \chi_{c0}(1P)$ process

The gluon-gluon fusion vertex is proportional to the reduced amplitude $\mathcal{T}_{\mu\nu}$ as follows,

$$\mathcal{V}_{\mu\nu}^{ab}(g^*g^* \rightarrow \chi_{c0}) = 4\pi\alpha_s \frac{\text{Tr}[t^a t^b]}{\sqrt{N_c}} 2\mathcal{T}_{\mu\nu} = \frac{4\pi\alpha_s}{\sqrt{N_c}} \delta^{ab} \mathcal{T}_{\mu\nu}, \quad (2.1)$$

$$\begin{aligned} \mathcal{T}_{\mu\nu} = & -\delta_{\mu\nu}^\perp(q_1, q_2) G_{\text{TT}}(q_1^2, q_2^2) \\ & + e_\mu^L(q_1) e_\nu^L(q_2) G_{\text{LL}}(q_1^2, q_2^2), \end{aligned} \quad (2.2)$$

where α_s is the strong coupling; $N_c = 3$ and t^a are the number of colors and $SU(3)$ group generators in QCD, respectively; and

$$\begin{pmatrix} G_{\text{TT}} \\ G_{\text{LL}} \end{pmatrix} = \begin{pmatrix} -|\mathbf{q}_1||\mathbf{q}_2| & (q_1 \cdot q_2) \\ (q_1 \cdot q_2) & -|\mathbf{q}_1||\mathbf{q}_2| \end{pmatrix} \begin{pmatrix} G_1 \\ G_2 \end{pmatrix}, \quad (2.3)$$

while the relevant kinematical variables are displayed in Fig. 1. Here, we have the projector on transverse polarization states

$$\begin{aligned} -\delta_{\mu\nu}^\perp(q_1, q_2) = & -g_{\mu\nu} + \frac{1}{X} ((q_1 \cdot q_2)(q_{1\mu}q_{2\nu} + q_{1\nu}q_{2\mu}) \\ & - q_1^2 q_{2\mu} q_{2\nu} - q_2^2 q_{1\mu} q_{1\nu}), \end{aligned} \quad (2.4)$$

with $X = (q_1 \cdot q_2)^2 - q_1^2 q_2^2$. The longitudinal polarization vectors read as follows:

$$\begin{aligned} e_\mu^L(q_1) = & \sqrt{\frac{-q_1^2}{X}} \left(q_{2\mu} - \frac{q_1 \cdot q_2}{q_1^2} q_{1\mu} \right), \\ e_\nu^L(q_2) = & \sqrt{\frac{-q_2^2}{X}} \left(q_{1\nu} - \frac{q_1 \cdot q_2}{q_2^2} q_{2\nu} \right). \end{aligned} \quad (2.5)$$

The convoluted form of reduced amplitude can be written as

$$\mathcal{T} = n_\nu^+ n_\mu^- \mathcal{T}_{\mu\nu} = |\mathbf{q}_1||\mathbf{q}_2| G_1(q_1^2, q_2^2) + (\mathbf{q}_1 \cdot \mathbf{q}_2) G_2(q_1^2, q_2^2), \quad (2.6)$$

in terms of the light-cone vectors $n_\nu^\pm = (1, 0, 0, \pm 1)$. The form factors here $G_i(q_1^2, q_2^2)$ have the integral representations in terms of the P -wave charmonia wave function $\psi_\chi(z, \mathbf{k})$ (see Ref. [9] for more details),

$$\begin{aligned}
G_1(\mathbf{q}_1^2, \mathbf{q}_2^2) &= |\mathbf{q}_1||\mathbf{q}_2| \frac{4m_c}{\mathbf{q}_2^2} \int \frac{dz d^2\mathbf{k}}{z(1-z)16\pi^3} \psi_\chi(z, \mathbf{k}) 2z(1-z)(2z-1) \left[\frac{1}{\mathbf{l}_A^2 + \varepsilon^2} - \frac{1}{\mathbf{l}_B^2 + \varepsilon^2} \right] \\
G_2(\mathbf{q}_1^2, \mathbf{q}_2^2) &= 4m_c \int \frac{dz d^2\mathbf{k}}{z(1-z)16\pi^3} \psi_\chi(z, \mathbf{k}) \left[\frac{1-z}{\mathbf{l}_A^2 + \varepsilon^2} + \frac{z}{\mathbf{l}_B^2 + \varepsilon^2} \right] \\
&\quad + \frac{4m_c}{\mathbf{q}_2^2} \int \frac{dz d^2\mathbf{k}}{z(1-z)16\pi^3} \psi_\chi(z, \mathbf{k}) 4z(1-z) \left[\frac{\mathbf{q}_2 \cdot \mathbf{l}_A}{\mathbf{l}_A^2 + \varepsilon^2} - \frac{\mathbf{q}_2 \cdot \mathbf{l}_B}{\mathbf{l}_B^2 + \varepsilon^2} \right], \tag{2.7}
\end{aligned}$$

where z is a c -quark (or \bar{c} -antiquark) momentum fraction; \mathbf{k} is the relative $c\bar{c}$ transverse momentum; m_c is the mass of the c -quark; and the shorthand notations

$$\begin{aligned}
\varepsilon^2 &= z(1-z)\mathbf{q}_1^2 + m_c^2, & \mathbf{l}_A &= \mathbf{k} - (1-z)\mathbf{q}_2, \\
\mathbf{l}_B &= \mathbf{k} + z\mathbf{q}_2 \tag{2.8}
\end{aligned}$$

have been introduced.

B. Light-cone amplitude for $g^*g^* \rightarrow \eta_c$ process

In Ref. [8], we introduced the covariant form of the vertex for the fusion of two off-shell gluons into the η_c meson,

$$\mathcal{V}_{\mu\nu}^{ab} = (-i)4\pi\alpha_s \epsilon_{\mu\nu\alpha\beta} q^\alpha q^\beta \frac{\delta^{ab}}{2\sqrt{N_c}} 2I(\mathbf{q}_1^2, \mathbf{q}_2^2), \tag{2.9}$$

where $I(\mathbf{q}_1^2, \mathbf{q}_2^2) = F_{\gamma^*\gamma^* \rightarrow \eta_c}(\mathbf{q}_1^2, \mathbf{q}_2^2)/(e_c^2 \sqrt{N_c})$, or in the convoluted form

$$\mathcal{V}^{ab} = (-i)4\pi\alpha_s \frac{\delta^{ab}}{\sqrt{N_c}} I(\mathbf{q}_1^2, \mathbf{q}_2^2) |\mathbf{q}_1||\mathbf{q}_2| \sin(\phi_1 - \phi_2), \tag{2.10}$$

with $(\phi_1 - \phi_2)$ being the angle between \mathbf{q}_1 and \mathbf{q}_2 . We then express $I(\mathbf{q}_1^2, \mathbf{q}_2^2)$ in terms of light-cone wave functions as follows [12],

$$\begin{aligned}
I(\mathbf{q}_1^2, \mathbf{q}_2^2) &= 4m_c \int \frac{dz d^2\mathbf{k}}{z(1-z)16\pi^3} \psi_\eta(z, \mathbf{k}) \\
&\quad \times \left\{ \frac{1-z}{(\mathbf{k} - (1-z)\mathbf{q}_2)^2 + z(1-z)\mathbf{q}_1^2 + m_c^2} \right. \\
&\quad \left. + \frac{z}{(\mathbf{k} + z\mathbf{q}_2)^2 + z(1-z)\mathbf{q}_1^2 + m_c^2} \right\}, \tag{2.11}
\end{aligned}$$

where $\psi_\eta(z, \mathbf{k})$ is the wave function of the $\eta_c(1S)$ meson.

III. MATRIX ELEMENT FOR $pp \rightarrow ppM$ REACTION

The amplitude for the CEP process for a given meson $V \equiv \chi_{c0}, \eta_c$ reads¹

¹Notice a factor 1/2 in the normalization, due to the fact that we use light-cone vectors fulfilling $n^+ \cdot n^- = 2$, matching the conventions of PST.

$$\begin{aligned}
\mathcal{M} &= \frac{s}{2} \pi^2 \frac{1}{2N_c^2 - 1} \int d^2\mathbf{Q} \mathcal{V}^{c_1 c_2} \\
&\quad \times \frac{\mathcal{F}_g^{\text{off}}(x_1, x', \mathbf{Q}^2, \mathbf{q}_1^2, \mu^2, t_1) \mathcal{F}_g^{\text{off}}(x_2, x', \mathbf{Q}^2, \mathbf{q}_2^2, \mu^2, t_2)}{\mathbf{Q}^2 \mathbf{q}_1^2 \mathbf{q}_2^2}, \tag{3.1}
\end{aligned}$$

in terms of the ‘‘active’’ (fusing into V) $x_{1,2}$ and ‘‘screening’’ x' (connecting both proton lines) gluon momentum fractions. The screening gluon carries a transverse momentum \mathbf{Q} , while the transverse momenta of active gluons are denoted by $\mathbf{q}_1, \mathbf{q}_2$. The generalized UGDs also depend on the hard scale of the process μ (see below). The $2 \rightarrow 3$ total cross section can be calculated generically as follows,

$$\begin{aligned}
\sigma &= \frac{1}{2s} \int |\mathcal{M}|^2 (2\pi)^4 \delta^4(p_1 + p_2 - p'_1 - p'_2 - p_V) \\
&\quad \times \left(\frac{1}{2(2\pi)^3} \right)^3 (dy'_1 d^2\mathbf{p}'_1) (dy'_2 d^2\mathbf{p}'_2) (dy d^2\mathbf{p}_V), \tag{3.2}
\end{aligned}$$

or, following a simplification done in Ref. [13], as

$$\sigma = \frac{1}{2s} \frac{1}{2^8 \pi^4 s} \int |\mathcal{M}|^2 dt_1 dt_2 dy d\phi. \tag{3.3}$$

Above, $t_1 = (p_1 - p'_1)^2$, $t_2 = (p_2 - p'_2)^2$, $\phi \in (0, 2\pi)$ is the relative azimuthal angle between the outgoing protons, s is the pp center-of-mass energy squared, and y is rapidity of the outgoing meson V .

IV. DIFFERENT APPROACHES TO OFF-DIAGONAL GLUON DENSITIES

In the forward limit of small $t_{1,2} \rightarrow 0$ corresponding to $\mathbf{Q}^2 \simeq \mathbf{q}_{1,2}^2 \equiv \mathbf{Q}_\perp^2$, the generalized UGDs in Eq. (3.1) are simplified and are considered as functions of only one transverse momentum, i.e.,

$$\mathcal{F}_g^{\text{off}}(x_1, x', \mathbf{Q}^2, \mathbf{q}_1^2, \mu^2, t_1) \rightarrow \mathcal{F}_g^{\text{off}}(x_1, x', \mathbf{Q}_\perp^2, \mu^2, t_1). \tag{4.1}$$

The Khoze-Martin-Ryskin (KMR) prescription for the off-diagonal (‘‘skewed’’) UGD includes a Sudakov form factor $T_g(\mathbf{q}_\perp^2, \mu^2)$ and is typically written as [1]

$$\begin{aligned} \mathcal{F}_{g,\text{KMR}}^{\text{off}}(x, x', Q_{\perp}^2, \mu^2; t) \\ = R_g \frac{d}{d \ln q_{\perp}^2} \left[xg(x, q_{\perp}^2) \sqrt{T_g(q_{\perp}^2, \mu^2)} \right]_{q_{\perp}^2 = Q_{\perp}^2} F(t), \end{aligned} \quad (4.2)$$

with gluon virtualities $q_{\perp}^2 \equiv \mathbf{q}^2$ playing a role of the momentum scale squared in the collinear gluon density $xg(x, q_{\perp}^2)$ and with the nucleon form factor $F(t)$ often parametrized in the following two ways,

$$\begin{aligned} F(t) &= \frac{4m_p^2 - 2.79t}{(4m_p^2 - t)(1 - t/0.71)^2} \quad \text{or} \\ F(t) &= \exp\left(\frac{bt}{2}\right), \quad b = 4 \text{ GeV}^{-2}, \end{aligned} \quad (4.3)$$

with m_p being the proton mass, corresponding to the isoscalar nucleon form factor [14] or the QCD elastic profile factor, respectively.

The Sudakov form factor is taken as

$$\begin{aligned} T_g(q_{\perp}^2, \mu^2) &= \exp\left[-\int_{q_{\perp}^2}^{\mu^2} \frac{dk_{\perp}^2}{k_{\perp}^2} \frac{\alpha_s(k_{\perp}^2)}{2\pi}\right] \\ &\times \int_0^{1-\Delta} \left[z P_{gg}(z) + \sum_q P_{qg}(z) \right] dz, \end{aligned} \quad (4.4)$$

with the hard scale $\mu^2 = M_V^2 + q_{\perp}^2$ and $\Delta = k_{\perp}/(k_{\perp} + \mu)$.

Regarding the longitudinal momentum fractions, central diffractive production is dominated by the region $x' \ll x_{1,2} \ll 1$. We thus compute the skewedness correction R_g in Eq. (4.2) using a method proposed and derived for the collinear off-diagonal gluon distributions [15]:

$$R_g = \frac{2^{2\lambda+3} \Gamma(\lambda + 5/2)}{\sqrt{\pi} \Gamma(\lambda + 4)}, \quad \lambda = \frac{d}{d \ln(1/x)} [\ln(xg(x, q_{\perp}^2))]. \quad (4.5)$$

In a slightly off-forward case $t_{1,2} \neq 0$, the choice of Q_{\perp} in the off-diagonal KMR gluon in Eq. (4.2) becomes somewhat arbitrary. In practical calculations, we use the so-called ‘‘minimum prescription’’ proposed by the Durham group, by substituting $Q_{\perp}^2 \rightarrow \min(Q_{\perp}^2, q_{\perp}^2)$ in Eq. (4.2), with transverse momentum of an active gluon q_{\perp} and transverse momentum of the screening gluon Q_{\perp} . In addition, we suggest a geometrical average of active and screening gluon momenta as $Q_{\perp}^2 \rightarrow \sqrt{Q_{\perp}^2 q_{\perp}^2}$ —an option, called Babiarz-Pasechnik-Schäfer-Szczurek (BPSS) in the following, for brevity.

We vary our results by also using the modified off-diagonal Cudell-Dechambre-Hernandez-Ivanov (CDHI) gluon defined as [16]

$$\begin{aligned} \mathcal{F}_{g,\text{CDHI}}^{\text{off}}(x, x', Q_{\perp}, \mu^2; t) \\ = R_g \left[\frac{\partial}{\partial \log \bar{Q}^2} \sqrt{T_g(\bar{Q}^2, \mu^2)} xg(x, \bar{Q}^2) \right] \cdot \frac{2Q_{\perp}^2 q_{\perp}^2}{Q_{\perp}^4 + q_{\perp}^4} \cdot F(t), \end{aligned} \quad (4.6)$$

where $\bar{Q}^2 = (Q_{\perp}^2 + q_{\perp}^2)/2$. In order to take into account the saturation effects, we use of the simplest saturation-based UGD inspired by the Golec-Biernat-Wüsthoff (GBW) model [17]. In order to extrapolate it into the off-diagonal domain, we use the prescription proposed in Ref. [3] (further referred to as the PST prescription),

$$\begin{aligned} \mathcal{F}_{g,\text{GBW}}^{\text{off}} &= \sqrt{Q_{\perp}^2 f_g^{\text{GBW}}(x', Q_{\perp}^2) q_{\perp}^2 f_g^{\text{GBW}}(x, q_{\perp}^2)} \\ &\times \sqrt{T_g(q_{\perp}^2, \mu^2)} F(t), \\ f_g^{\text{GBW}}(x, q_{\perp}^2) &= \frac{3\sigma_0}{4\pi^2 \alpha_s} R_0^2 q_{\perp}^2 \exp[-R_0^2 q_{\perp}^2], \end{aligned} \quad (4.7)$$

where f_g^{GBW} is the diagonal GBW UGD and $x' = |\mathbf{Q}|/\sqrt{s}$, $R_0 = (x/x_0)^{\lambda/2}$. In practical calculations, we have used the following fitted values of the GBW parameters obtained by Golec-Biernat and Sapeta [18]: $\sigma_0 = 29.12 \text{ mb}$, $\lambda = 0.277$, $x_0/10^{-4} = 0.41$, with $\alpha_s(q_{\perp}^2) = \min(0.82, \frac{4\pi}{9 \log(Q^2/\Lambda_{\text{QCD}}^2)})$ and $Q^2 = \max(q_{\perp}^2, 0.22 \text{ GeV}^2)$, $\Lambda_{\text{QCD}}^2 = 0.04 \text{ GeV}^2$.

As an alternative model based on the color dipole cross section, we used a fit obtained by Rezaeian and Schmidt [19]. While the GBW model resembles the eikonal unitarization, the Rezaeian-Schmidt (RS) cross section uses a form of the dipole cross section proposed in Ref. [20] which is motivated by the Balitsky-Fadin-Kuraev-Lipatov equation and its nonlinear generalizations. We computed the corresponding UGD $f_g^{\text{RS}}(x, |\mathbf{q}|)$ as

$$f_g^{\text{RS}}(x, |\mathbf{q}|) = \mathbf{q}^2 \frac{\sigma_0 N_c}{\alpha_s 8\pi^2} \int_0^{\infty} r dr J_0(|\mathbf{q}|r) \left(1 - \frac{\sigma(x, r)}{\sigma_0}\right). \quad (4.8)$$

As an example, we have used the first set of parameters from Table I in Ref. [19].

V. NUMERICAL RESULTS

In the CEP processes at high energies, it is mandatory to consider gluons carrying very small longitudinal momentum fractions x . For this purpose, in practical calculations, we use a few parton distribution functions (PDFs): JR14NLO [21] ($Q_{0T}^2 = 0.8 \text{ GeV}^2$), GJR08NLO [22] ($Q_{0T}^2 = 0.5 \text{ GeV}^2$), and GRV94NLO [23] ($Q_{0T}^2 = 0.4 \text{ GeV}^2$). In Fig. 2, we illustrate the shape of the corresponding gluon PDFs at scales and longitudinal momenta fractions typical for the considered $pp \rightarrow pp\eta_c$ and $pp \rightarrow pp\chi_{c,0}$ CEP processes. In the range of scales under discussion, the gluon PDFs from the literature differ considerably. We do not employ the Durham or CTEQ PDFs for which the initial scales for evolution are rather high, making them difficult to apply in the context of the exclusive reactions discussed here.

The total cross sections computed over the full phase space for each PDF mentioned above are listed in

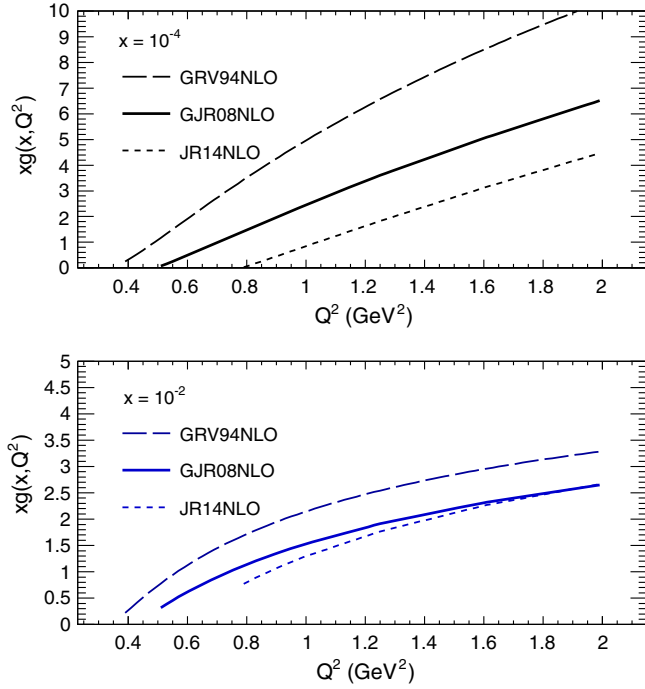


FIG. 2. Collinear gluon PDF as a function of the hard scale of the process and for typical longitudinal gluon momentum fractions, $x = 10^{-4}$ (upper plot) and $x = 10^{-2}$ (lower plot).

Tables I and II, for χ_{c0} and η_c , respectively. The integrated cross section for $pp \rightarrow pp\chi_{c0}$ at $\sqrt{s} = 13$ TeV is shown in Table I for different off-diagonal UGD prescriptions for the effective Q_{iT}^2 summarized as follows:

- Durham prescription [Eq. (4.2)]: $Q_{iT}^2 = \min(Q_T^2, q_{iT}^2)$,
- BPSS prescription [Eq. (4.2)]: $Q_{iT}^2 = \sqrt{Q_T^2 q_{iT}^2}$,
- CDHI prescription [Eq. (4.6)]: $Q_{iT}^2 = (Q_T^2 + q_{iT}^2)/2$,
- PST off-diagonal UGD [Eq. (4.7)].

For χ_c production, these prescriptions lead to similar cross sections of the order of $1 \mu\text{b}$ before including absorption effects. The corresponding gap survival factor is of the order of 0.1 as will be discussed at the end of this section.

In Table II, we present similar results for η_c production. The total cross section for the η_c production is 3–4 orders of magnitude smaller than that for χ_{c0} , i.e., surprisingly small. The cross section for the PST prescription for off-diagonal gluon is quite similar as for the Durham and CDHI prescriptions in the case of χ_{c0} , while the spread in the total cross section for η_c is much higher.

In Fig. 3, we show the rapidity distribution of χ_{c0} (left) and η_c (right) quarkonia CEP. We show results for the Durham (min) and CDHI prescription for the off-diagonal unintegrated gluon distributions (UGDs). We present results for $R_g = 1$ as well as with R_g calculated according to the Shuvaev prescription [see Eq. (4.5)]. Inclusion of R_g increases the cross section by a factor of 3–4. While for χ_{c0} the difference of the results for the Durham prescription and

TABLE I. Total cross section for χ_{c0} at $\sqrt{s} = 13$ TeV with $R_g = 1.0$ and R_g according to Eq. (4.5). In order to obtain the cross section, several gluon distributions were used with $Q_{0T}^2 \geq 0.4$ GeV² for GRV94NLO, $Q_{0T}^2 \geq 0.5$ GeV² for GJR08NLO, and $Q_{0T}^2 \geq 0.8$ GeV² for JR14NLO. The light-cone form factor for the $gg \rightarrow \chi_{c0}$ coupling was calculated using the Buchmüller-Tye potential (for more details, see Ref. [9]) No gap survival factor is included here.

KMR skewed gluon $0.8 \text{ GeV}^2 \leq Q_{0T}^2$, JR14NLO	σ_{tot} (nb), $R_g = 1.0$	σ_{tot} (nb), $R_g(x, Q_{iT}^2)$
CDHI, $Q_{iT}^2 = (Q_T^2 + q_{iT}^2)/2$.	0.42×10^3	1.1×10^3
KMR, $Q_{iT}^2 = \sqrt{Q_T^2 \cdot q_{iT}^2}$	0.36×10^3	0.94×10^3
KMR, $Q_{iT}^2 = \min(Q_T^2, q_{iT}^2)$	0.20×10^3	0.52×10^3
KMR skewed gluon $0.5 \text{ GeV}^2 \leq Q_{0T}^2$, GJR08NLO	σ_{tot} (nb), $R_g = 1.0$	σ_{tot} (nb), $R_g(x, Q_{iT}^2)$
CDHI, $Q_{iT}^2 = (Q_T^2 + q_{iT}^2)/2$.	0.46×10^3	1.57×10^3
KMR, $Q_{iT}^2 = \sqrt{Q_T^2 \cdot q_{iT}^2}$	0.64×10^3	2.1×10^3
KMR, $Q_{iT}^2 = \min(Q_T^2, q_{iT}^2)$	0.34×10^3	1.1×10^3
KMR skewed gluon $0.4 \text{ GeV}^2 \leq Q_{0T}^2$, GRV94NLO	σ_{tot} (nb), $R_g = 1.0$	σ_{tot} (nb), $R_g(x, Q_{iT}^2)$
CDHI, $Q_{iT}^2 = (Q_T^2 + q_{iT}^2)/2$.	1.88×10^3	9.02×10^3
KMR, $Q_{iT}^2 = \sqrt{Q_T^2 \cdot q_{iT}^2}$	3.03×10^3	13.4×10^3
KMR, $Q_{iT}^2 = \min(Q_T^2, q_{iT}^2)$, $0.4 \text{ GeV}^2 \leq Q_{0T}^2$	1.4×10^3	6.1×10^3
KMR, $Q_{iT}^2 = \min(Q_T^2, q_{iT}^2)$, $0.8 \text{ GeV}^2 \leq Q_{0T}^2$	0.75×10^3	3.9×10^3
PST skewed gluon	σ_{tot} (nb)	...
PST prescription, GBW	0.44×10^3	...
PST prescription, RS	0.52×10^3	...

the CDHI prescription is small, for η_c , the difference is of the order of magnitude size.

The distribution in transverse momentum is shown in Fig. 4. The distribution for η_c and χ_{c0} CEP are somewhat different. The maximum of the cross section for η_c is at $p_T \sim 1$ GeV, and the dip at vanishing p_T is more pronounced.

In Fig. 5, we show two-dimensional distributions in (t_1, t_2) (t_1, t_2 are 4-momenta squared transferred in the proton lines), for the $pp \rightarrow pp\eta_c(1S)$ CEP process at $\sqrt{s} = 13$ TeV. Here, we present results for several prescriptions for the off-diagonal KMR UGDFs: with the Durham prescription (left-upper panel), the BPSS prescription (right-upper panel), and the CDHI prescription (left-lower panel) as well as the PST prescription for off-diagonal UGD using the diagonal GBW UGDF (right-lower panel). No gap survival effect is incorporated here. The results appear to be reasonably stable with respect to a change in the UGDs modeling, while the BPSS prescription differs in the distribution shape.

TABLE II. The same as in Table I but for the η_c meson. The light-cone form factor for the $gg \rightarrow \eta_c(1S)$ coupling was calculated using the power-law potential (for more details, see Ref. [8]).

KMR skewed gluon, $0.8 \text{ GeV}^2 \leq Q_{0T}^2$, JR14NLO	σ_{tot} (nb), $R_g = 1.0$	σ_{tot} (nb), $R_g(x, Q_{iT}^2)$
CDHI, $Q_{iT}^2 = (Q_T^2 + q_{iT}^2)/2$.	1.1	2.4
KMR, $Q_{iT}^2 = \sqrt{Q_T^2 \cdot q_{iT}^2}$	0.39	1.2
KMR, $Q_{iT}^2 = \min(Q_T^2, q_{iT}^2)$	0.13	0.25
KMR skewed gluon, $0.5 \text{ GeV}^2 \leq Q_{0T}^2$, GJR08NLO	σ_{tot} (nb), $R_g = 1.0$	σ_{tot} (nb), $R_g(x, Q_{iT}^2)$
CDHI, $Q_{iT}^2 = (Q_T^2 + q_{iT}^2)/2$.	2.2	5.6
KMR, $Q_{iT}^2 = \sqrt{Q_T^2 \cdot q_{iT}^2}$	0.52	2.1
KMR, $Q_{iT}^2 = \min(Q_T^2, q_{iT}^2)$, $0.5 \text{ GeV}^2 \leq Q_{0T}^2$	0.44	1.3
KMR, $Q_{iT}^2 = \min(Q_T^2, q_{iT}^2)$, $0.8 \text{ GeV}^2 \leq Q_{0T}^2$	0.22	0.45
KMR skewed gluon, $0.4 \text{ GeV}^2 \leq Q_{0T}^2$, GRV94NLO	σ_{tot} (nb), $R_g = 1.0$	σ_{tot} (nb), $R_g(x, Q_{iT}^2)$
CDHI, $Q_{iT}^2 = (Q_T^2 + q_{iT}^2)/2$.	1.2×10^2	7.8×10^3
KMR, $Q_{iT}^2 = \sqrt{Q_T^2 \cdot q_{iT}^2}$	2.2	1.3×10^3
KMR, $Q_{iT}^2 = \min(Q_T^2, q_{iT}^2)$, $0.4 \text{ GeV}^2 \leq Q_{0T}^2$	2.8	1.0×10^1
KMR, $Q_{iT}^2 = \min(Q_T^2, q_{iT}^2)$, $0.8 \text{ GeV}^2 \leq Q_{0T}^2$	1.25	2.9
PST skewed gluon	σ_{tot} (nb)	...
PST, GBW	1.9	...
PST, RS	4.1	...

For completeness, in Fig. 6, we show similar results for the χ_{c0} production. In this case, all prescriptions for effective transverse momenta (Durham, BPSS, and CDHI

prescriptions) lead to fairly similar results. Here, the cross sections are peaked at $t_1 = 0$, $t_2 = 0$.

In Fig. 7, we show relative azimuthal angle (between outgoing protons) distributions. The distribution for χ_{c0} (left) is very different than that for η_c (right). While for χ_{c0} there is one maximum for the back-to-back configurations, there are two maxima for η_c . The cross section vanishes in the back-to-back kinematics in the case of η_c CEP. The exact position of the maxima depends on the details of the treatment of the off-diagonal UGDs, so their experimental identification could pin down the correct theoretical modeling of these objects.

Finally, we wish to compare our results for the exclusive reactions $pp \rightarrow pp\eta_c$ and $pp \rightarrow pp\chi_{c0}$ with their inclusive production counterparts as calculated recently in Refs. [8,9]. In Figs. 8 and 9, we show the numerical results (rapidity and transverse momentum distributions) for η_c and χ_{c0} , respectively. While for η_c production the cross section for the exclusive process is a few orders of magnitude lower than that for the inclusive case, this is quite different for the χ_{c0} meson. Both for rapidity and transverse momentum distributions, the results for the exclusive case are very different compared to the inclusive case.

The two UGDs obtained from the dipole cross section, labeled GBW and RS, give rise to similar distributions. For the case of η_c , the RS UGD gives a larger cross section than that obtained with the GBW model, while in the case of χ_c , their sizes are very similar.

VI. ABSORPTIVE CORRECTIONS

It is understood that the Born-level cross sections receive absorptive corrections through hadronic rescatterings at large distances. These are related to the interactions of spectator partons [24]. They give rise to the so-called gap survival probability in exclusive reactions. The calculation

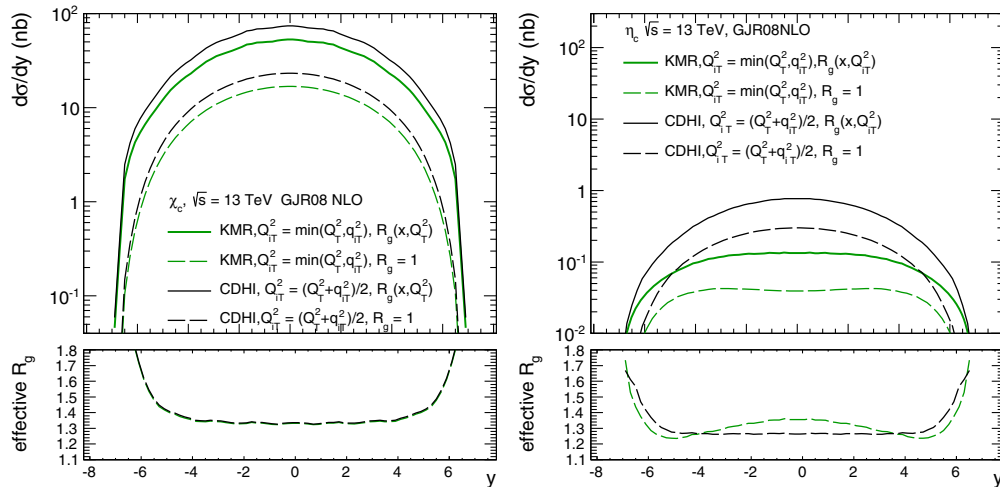


FIG. 3. The rapidity distribution for χ_{c0} , η_c quarkonia CEP and effective R_g factor calculated with the GJR08NLO parton distribution function. No gap survival factor is included here.

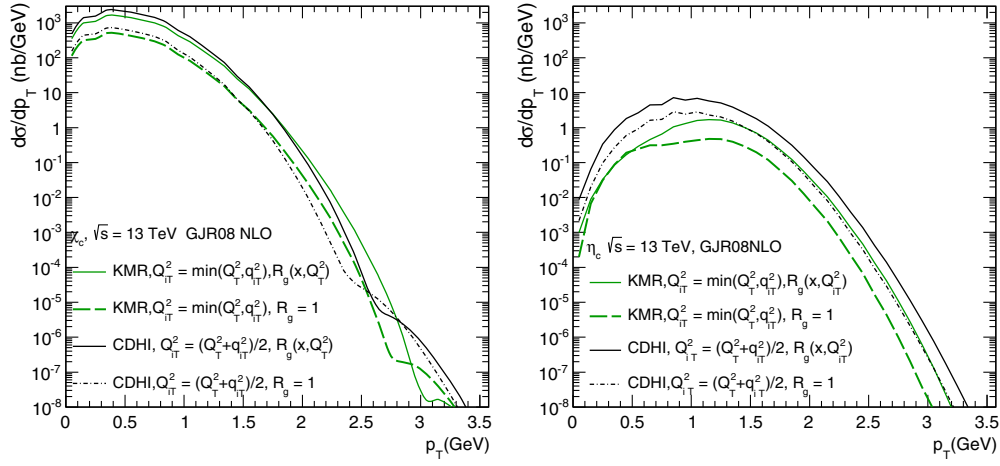


FIG. 4. Distribution in transverse momentum of the χ_{c0} (left) and η_c (right) quarkonia CEP, respectively, with different treatment of R_g factor. No gap survival factor is included here.

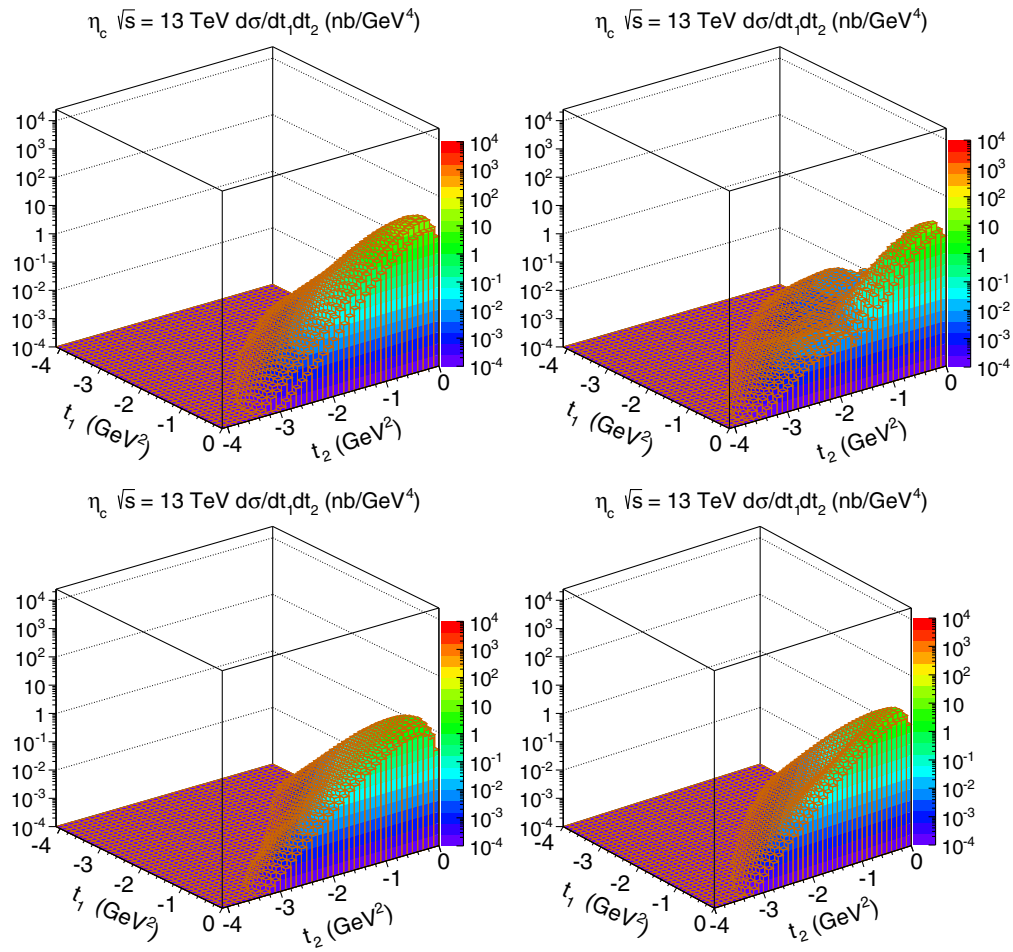


FIG. 5. Distribution in $t_1 \times t_2$ for CDHI (left upper), BPSS (right upper), and Durham (left lower) prescriptions calculated with the GJR08NLO gluon distribution function and for the PST off-diagonal UGD computed with the diagonal GBW UGD (right lower) for η_c CEP for $\sqrt{s} = 13$ TeV. No gap survival factor is included here.

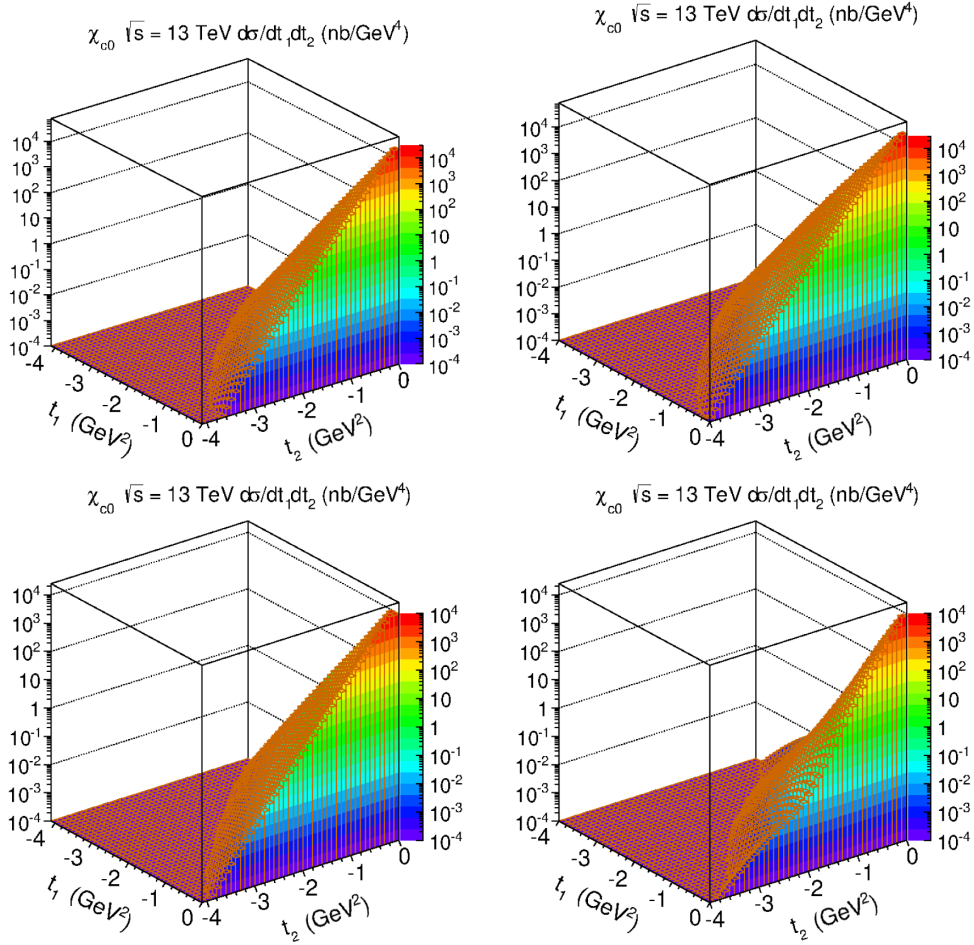


FIG. 6. Distribution in $t_1 \times t_2$ for CDHI (left upper), BPSS ($Q_{IT}^2 = \sqrt{q_{IT}^2, Q_T^2}$) (right upper), and Durham [$Q_{IT}^2 = \min(q_{IT}^2, Q_T^2)$] (left lower) prescriptions calculated with the GJR08NLO gluon distribution function and for the PST off-diagonal UGD computed with the diagonal GBW UGD (right lower) for χ_{c0} for $\sqrt{s} = 13$ TeV. No gap survival factor is included here.

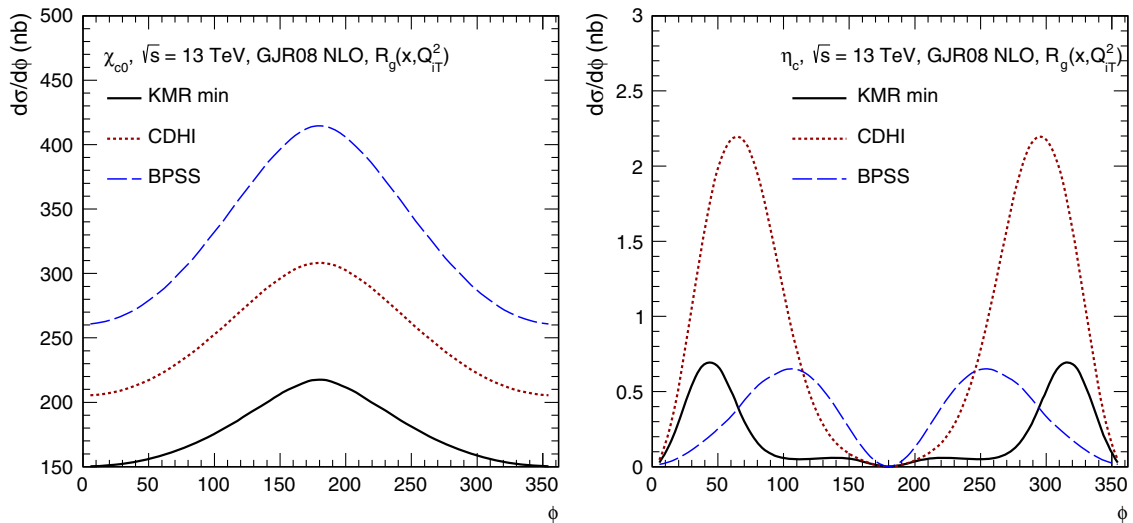


FIG. 7. Distribution in relative azimuthal angle between outgoing protons, for χ_{c0} (left panel) and for η_c (right panel), using different prescriptions for UGDs. No gap survival factor is included here.

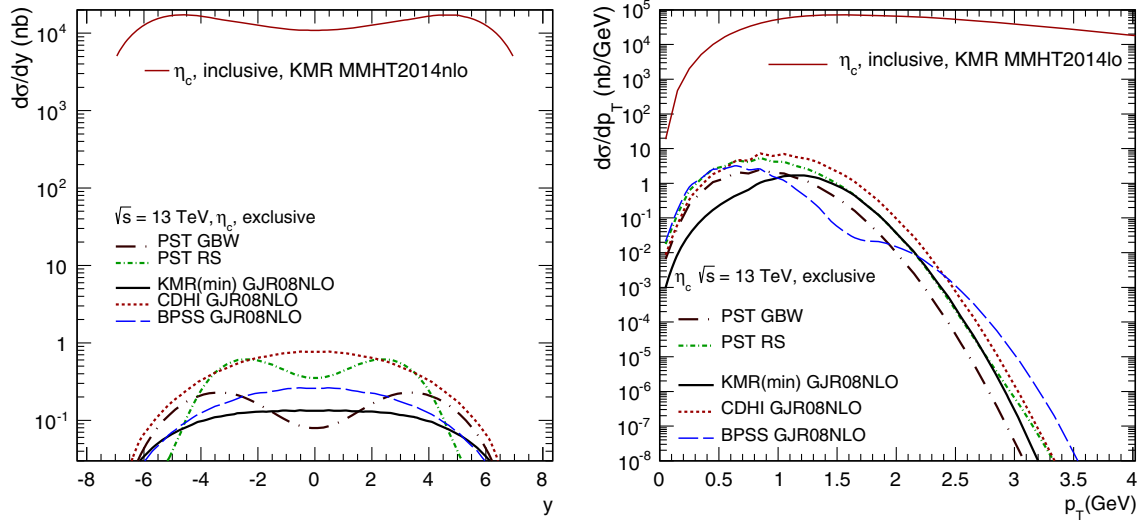


FIG. 8. Comparison of exclusive and inclusive η_c production at $\sqrt{s} = 13$ TeV. No gap survival factor is included for the exclusive reaction.

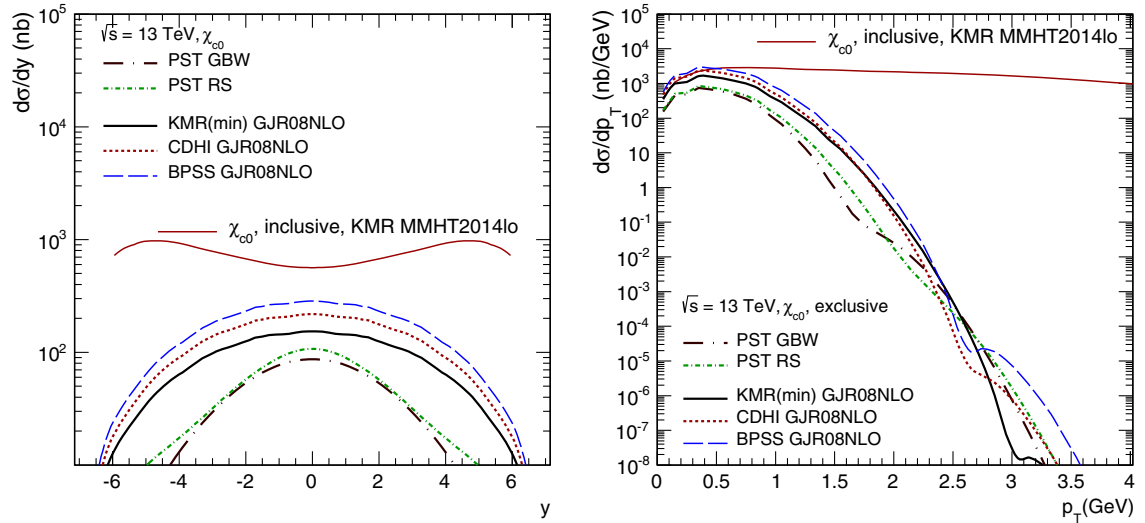


FIG. 9. Comparison of exclusive and inclusive χ_{c0} production at $\sqrt{s} = 13$ TeV. No gap survival factor is included for the exclusive reaction.

of the latter poses a difficult problem, which has not been solved yet in a way fully consistent with the perturbative QCD approach to the production amplitude.

Numerous approaches exist in the literature; some of them are based on soft multi-Pomeron exchanges [25–27], while other approaches avoid the decomposition into Born term and absorptive correction altogether, treating the absorptive effects dynamically [28,29] and at the amplitude level in the dipole picture [30–32], and some of them relate the gap survival probability to the absence of multiparton interactions [33,34].

It is also understood that the gap survival must depend on the kinematics of the process. Here, we wish to discuss the absorptive corrections at the amplitude level, in a simple

quantum-mechanical treatment. To this end, we adopt a simple effective Reggeon Field Theory motivated approach.

In the simplified case where only “elastic rescattering” is taken into account, the amplitude looks as follows:

$$\mathcal{M}(Y, y, \mathbf{p}_1, \mathbf{p}_2) = \mathcal{M}^{(0)}(Y, y, \mathbf{p}_1, \mathbf{p}_2) - \delta\mathcal{M}(Y, y, \mathbf{p}_1, \mathbf{p}_2). \quad (6.1)$$

Here, $Y = \log(s/m_p^2)$ is the rapidity difference between the colliding beams at center-of-mass energy \sqrt{s} , y is the c.m. rapidity of the produced meson V , and $\mathbf{p}_{1,2}$ are the transverse momenta of outgoing protons.

The absorptive correction is then computed as follows,

$$\delta\mathcal{M}(Y, y, \mathbf{p}_1, \mathbf{p}_2) = \int \frac{d^2\mathbf{k}}{2(2\pi)^2} T(s, \mathbf{k}) \mathcal{M}^{(0)}(Y, y, \mathbf{p}_1 + \mathbf{k}, \mathbf{p}_2 - \mathbf{k}), \quad (6.2)$$

with

$$T(s, \mathbf{k}) = \sigma_{\text{tot}}^{pp}(s) \exp\left(-\frac{1}{2} B_{\text{el}}(s) \mathbf{k}^2\right). \quad (6.3)$$

At $\sqrt{s} = 13$ TeV, we take $\sigma_{\text{tot}}^{pp} = (110.6 \pm 3.4)$ mb and the nuclear slope $B_{\text{el}} = (20.36 \pm 0.19)$ GeV⁻² [35]. In a double-Regge approach, the Born-level amplitude has the form

$$\mathcal{M}^{(0)}(Y, y, \mathbf{p}_1, \mathbf{p}_2) = is\Phi_1(\mathbf{p}_1) R_{\text{IP}}(Y - y, \mathbf{p}_1^2) V(\mathbf{p}_1, \mathbf{p}_2) R_{\text{IP}}(y, \mathbf{p}_2^2) \Phi_2(\mathbf{p}_2). \quad (6.4)$$

Here, $R_{\text{IP}}(y, \mathbf{p}^2)$ are the Pomeron Regge-propagators, and $V(\mathbf{p}_1, \mathbf{p}_2)$ is the **IPIP** → meson vertex.

Let us now briefly discuss the vertices $V(\mathbf{p}_1, \mathbf{p}_2)$. The most general form of the Pomeron-Pomeron-particle vertex for a spinless particle can be written as a Fourier expansion:

$$V(\mathbf{p}_1, \mathbf{p}_2) = V_0(\mathbf{p}_1^2, \mathbf{p}_2^2) + \sum_{n \geq 1} (V_n^+(\mathbf{p}_1^2, \mathbf{p}_2^2) \cos(n\phi) + V_n^-(\mathbf{p}_1^2, \mathbf{p}_2^2) \sin(n\phi)). \quad (6.5)$$

For a scalar particle, all $V_n^- = 0$, while for the pseudoscalar $V_0 = 0, V_n^+ = 0$. For definiteness, let us concentrate on only the first order, $n = 1$. We thus adopt (V^{0+} for the scalar and V^{0-} for the pseudoscalar state):

$$V^{0+}(\mathbf{p}_1, \mathbf{p}_2) = V_0 + V_1^+(\mathbf{p}_1 \cdot \mathbf{p}_2) = V_0(1 + \tau B_D(\mathbf{p}_1 \cdot \mathbf{p}_2))$$

$$\text{with } \tau \equiv \frac{V_1^+}{B_D V_0}$$

$$V^{0-}(\mathbf{p}_1, \mathbf{p}_2) = V_1^-[\mathbf{p}_1, \mathbf{p}_2]. \quad (6.6)$$

We further neglect a possible dependence of vertices V_i^\pm on \mathbf{p}_1^2 and \mathbf{p}_2^2 .

Our amplitude is normalized in such a way that the expression

$$d\sigma = \frac{1}{256\pi^5 s^2} |\mathcal{M}(Y, y, \mathbf{p}_1, \mathbf{p}_2)|^2 dy d^2\mathbf{p}_1 d^2\mathbf{p}_2 d^2\mathbf{p} \times \delta^{(2)}(\mathbf{p} + \mathbf{p}_1 + \mathbf{p}_2) \quad (6.7)$$

holds. We will now concentrate on central diffractive production; i.e., we fix the meson rapidity to be $y = 0$. Below, we adopt $\sqrt{s} = 13$ TeV. We can therefore forget about the Regge propagators in Eq. (6.4), and without loss of generality, we write

$$\Phi_{1,2}(\mathbf{p}_{1,2}) = \exp\left(-\frac{1}{2} B_D \mathbf{p}_{1,2}^2\right). \quad (6.8)$$

Then, using the vertices of Eq. (6.6), the transverse momentum distributions of the mesons at the Born level are obtained as

$$\left. \frac{d\sigma_{\text{Born}}^{0+}}{dy d^2p_T^2} \right|_{y=0} = \frac{\exp[-\frac{1}{2} B_D p_T^2] V_0^2}{512\pi^3 B_D} \left\{ 1 - \tau \left(1 - \frac{1}{2} B_D p_T^2 \right) + \frac{\tau^2}{2} \left(1 - \frac{1}{2} B_D p_T^2 + \frac{1}{8} B_D^2 p_T^4 \right) \right\}$$

$$\left. \frac{d\sigma_{\text{Born}}^{0-}}{dy d^2p_T^2} \right|_{y=0} = \frac{(V_1^-)^2 p_T^2}{512\pi^3 4B_D^2} \exp\left[-\frac{1}{2} B_D p_T^2\right]. \quad (6.9)$$

Now, the absorptive corrections require the evaluation of the loop integral

$$\delta\mathcal{M}(Y, 0, \mathbf{p}_1, \mathbf{p}_2) = \int \frac{d^2\mathbf{k}}{2(2\pi)^2} T(s, \mathbf{k}) \exp\left(-\frac{1}{2} B_D(\mathbf{p}_1 + \mathbf{k})^2\right) \exp\left(-\frac{1}{2} B_D(\mathbf{p}_2 - \mathbf{k})^2\right)$$

$$\times V(\mathbf{p}_1 + \mathbf{k}, \mathbf{p}_2 - \mathbf{k}) = \exp\left(-\frac{1}{2} B_D(\mathbf{p}_1^2 + \mathbf{p}_2^2)\right)$$

$$\times \int \frac{d^2\mathbf{k}}{2(2\pi)^2} \exp\left(-\frac{1}{2} (B_{\text{el}}(s) + 2B_D) \mathbf{k}^2 - B_D \mathbf{k} \cdot (\mathbf{p}_1 - \mathbf{p}_2)\right) \sigma_{\text{tot}}^{pp}(s) V(\mathbf{p}_1 + \mathbf{k}, \mathbf{p}_2 - \mathbf{k}). \quad (6.10)$$

It is useful to introduce the dimensionless quantities

$$g_{\text{abs}} = \frac{\sigma_{\text{tot}}^{pp}(s)}{4\pi(B_{\text{el}}(s) + 2B_D)} \quad \text{and} \quad \beta = \frac{B_D}{B_{\text{el}}(s) + 2B_D}. \quad (6.11)$$

TABLE III. V_0 and τ at midrapidity of χ_{c0} , for several prescriptions for off-diagonal UGDs.

χ_{c0}	V_0^+ ($\sqrt{\text{nb}}/\text{GeV}^2$)	τ	B_D (GeV^{-2})	g_{abs}	β	$\sigma_{\text{tot}} _{y=0}$ (nb)	$\sigma_{\text{tot}}^{\text{abs}} _{y=0}$ (nb)	$S_{y=0}^2$
PST GBW	-2062	-0.31	5.7	0.71	0.18	17	3.7	0.21
PST RS	-2381	-0.28	5.9	0.70	0.18	21	4.5	0.21
CDHI GJR08NLO	-2985	-0.135	4.5	0.76	0.15	42	7.5	0.18
KMR GJR08NLO	-2167	-0.11	4.5	0.77	0.15	29	3.7	0.13
BPSS GJR08NLO	-3118	-0.135	4.5	0.77	0.15	61	8.0	0.13

TABLE IV. An example of V_1 values at midrapidity of η_c in the CEP process, for several prescriptions for off-diagonal UGDs.

η_c	V_1^- ($\sqrt{\text{nb}}/\text{GeV}^4$)	B_D (GeV^{-2})	g_{abs}	β	$\sigma_{\text{tot}} _{y=0}$ (nb)	$\sigma_{\text{tot}}^{\text{abs}} _{y=0}$ (nb)	$S_{y=0}^2$
PST GBW	194	3.4	0.83	0.12	1.8×10^{-2}	3.9×10^{-3}	0.21
PST RS	400	3.2	0.84	0.12	9.0×10^{-3}	1.9×10^{-3}	0.21
CDHI GJR08NLO	651	3.5	0.81	0.13	1.8×10^{-1}	4.0×10^{-2}	0.22
KMR GJR08NLO	1015	4.7	0.76	0.16	1.3×10^{-1}	3.0×10^{-2}	0.29
BPSS GJR08NLO	1490	7.0	0.66	0.20	5.8×10^{-2}	2.2×10^{-2}	0.38

Then, at small $\mathbf{p}_1^2, \mathbf{p}_2^2$, the absorptive corrections are obtained as

$$\begin{aligned} \delta\mathcal{M}^{0+}(Y, 0, \mathbf{p}_1, \mathbf{p}_2) &= g_{\text{abs}} V_0 \exp\left(-\frac{1}{2} B_D (\mathbf{p}_1^2 + \mathbf{p}_2^2)\right) \exp\left(\frac{1}{2} \beta B_D (\mathbf{p}_1 - \mathbf{p}_2)^2\right) \\ &\times \{1 + \beta(1 + \beta) \tau B_D (\mathbf{p}_1^2 + \mathbf{p}_2^2) + (\mathbf{p}_1 \cdot \mathbf{p}_2) \tau B_D (1 - 2\beta(1 + \beta))\}, \end{aligned} \quad (6.12)$$

$$\begin{aligned} \delta\mathcal{M}^{0-}(Y, 0, \mathbf{p}_1, \mathbf{p}_2) &= (1 - \beta) g_{\text{abs}} V_1^- \exp\left(-\frac{1}{2} B_D (\mathbf{p}_1^2 + \mathbf{p}_2^2)\right) \exp\left(\frac{1}{2} \beta B_D (\mathbf{p}_1 - \mathbf{p}_2)^2\right) \\ &\times [\mathbf{p}_1, \mathbf{p}_2] (1 - \beta) (1 - \beta B_D (\mathbf{p}_1 \cdot \mathbf{p}_2)), \end{aligned} \quad (6.13)$$

for the scalar and pseudoscalar meson, respectively. We now adjust the constants V_0, V_1^\pm , as well as B_D , to our numerical results obtained for the Born-level amplitude.

In Tables III and IV, we show the parameters obtained for different prescriptions for the generalized unintegrated gluon distribution, GBW, as well as the CDHI and Durham prescriptions for the GJR08NLO gluon distribution. We also show the gap survival factors

$$S^2 \equiv \frac{d\sigma/dy|_{y=0}}{d\sigma_{\text{Born}}/dy|_{y=0}}. \quad (6.14)$$

We observe that, depending on the gluon distribution used, we obtain for the χ_c the gap survival values of $S^2 = 0.13 \div 0.21$, while for the η_c production, they are systematically somewhat higher, $S^2 = 0.21 \div 0.38$. Notice that the η_c amplitude, due to the vanishing in forward direction, is more peripheral than the one for χ_c production. However, also notice that the both reactions have significantly different values of the effective diffraction slopes B_D . Regarding the diffraction slope, we furthermore observe a strong model dependence, especially for the η_c case.

Our simplified double-Regge approach works reasonably well. In Fig. 10, we show the cross section $d\sigma/dydp_T$ at $y = 0$ for the χ_c for the three different generalized UGD prescriptions. Shown is the exact numerical result of the Born amplitude (solid line) as well as the result of our effective Regge amplitude fit (long-dashed line). By the short-dashed line, we show the differential cross section including absorptive corrections on top of the Regge amplitude Born term. We see from these figures that the effective Regge amplitude form is reasonably accurate for $p_T \lesssim 1.5$ GeV, with a slight ambiguity in the slope B_D . In the case of the η_c shown in Fig. 11, the effective Regge fit works almost perfectly for the PST-GBW and CDHI prescriptions, while for the Durham case, the description is rather poor.

In our calculation of absorptive corrections, we restricted ourselves to the so-called elastic rescattering correction. We wish to point out that the often applied multichannel models that account for the possible diffractively excited intermediate states, are constructed for soft diffractive processes. In our case, we deal with a Born-level processes with (semi)hard gluon exchanges, which will favor a

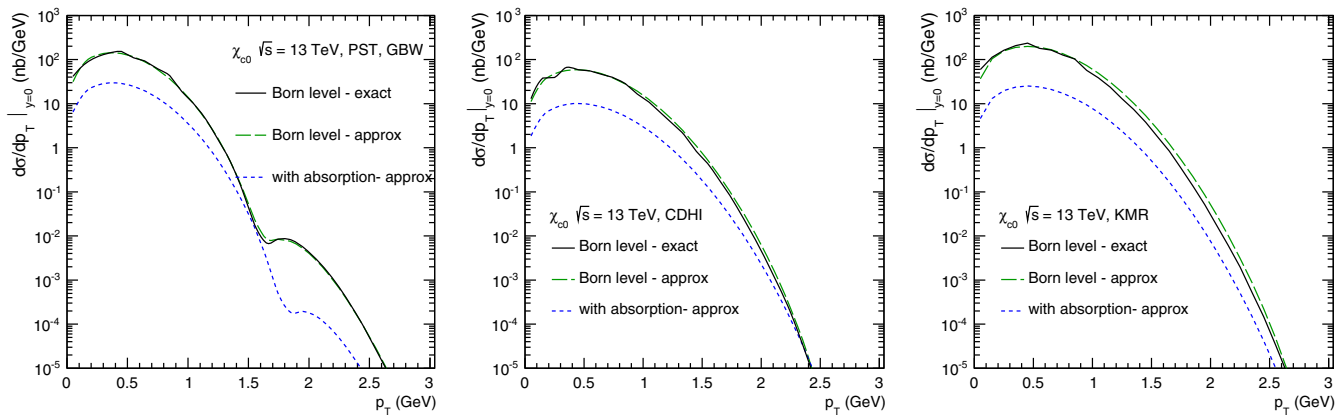


FIG. 10. Transverse momentum distribution of χ_{c0} CEP at $y = 0$, with the PST-GBW, the CDHI, and Durham prescription.

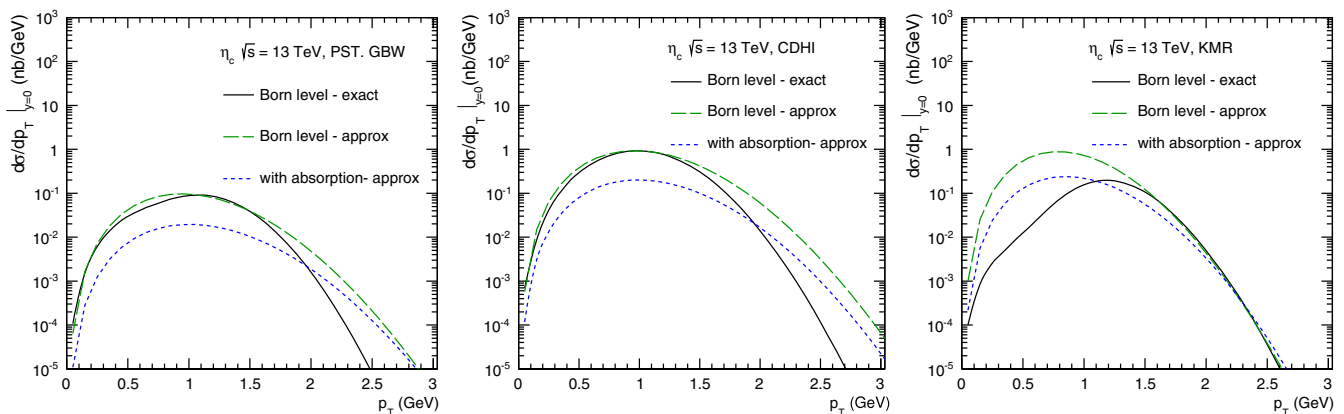


FIG. 11. Distribution in transverse momentum of η_c in the CEP process for PST-GBW, CDHI, and Durham prescriptions at $y = 0$.

coupling to small color dipoles in each proton. It is not clear that the diffractive final states that dominate soft diffractive dissociation at the LHC have a large overlap with the relevant dipole sizes.

In this regard, we wish to point to the work of Refs. [30–32]. In these works, it is argued that for certain hard inclusive diffractive processes (part of) the rescattering corrections are in fact already included effectively in the dipole cross section. The consistent formalism for exclusive channels remains an important task for the future.

VII. CONCLUSION

In the present paper, we have calculated the key observables of central exclusive χ_{c0} and η_c quarkonia production in proton-proton collisions at the LHC within a formalism proposed earlier by the Durham group for central exclusive Higgs boson production.

The χ_{c0} meson CEP was already computed in the literature previously, while η_c production has been analysed here for the first time. Compared to the previous calculations, we have used here modern versions of collinear

gluon distributions to generate off-diagonal unintegrated gluon distributions.

In the present analysis, we have also used the $gg \rightarrow \eta_c$ and $gg \rightarrow \chi_{c0}$ transition amplitudes calculated using the light-cone $c\bar{c}$ wave functions obtained in the framework of potential models. We have performed similar calculations for inclusive production of η_c and χ_{c0} very recently and showed that one can very well describe the experimental data for the $\eta_c(1S)$ meson measured in last few years by the LHCb Collaboration. Our previous results showed that in the inclusive case the cross section for η_c is significantly larger than that for χ_{c0} .

It was the main aim of the present paper to make a similar analysis for the exclusive production case, which for the case of η_c has not been done so far in the literature. In contrast to the inclusive case, we have found that for the CEP the situation reverses; i.e., the corresponding cross section for exclusive η_c production is considerably smaller than its counterpart for exclusive χ_{c0} production, at least, for the hard part obtained using the Durham or Cudell *et al.* prescriptions for calculation of the scale in the off-diagonal unintegrated gluon distribution. The reason is a specific

interplay of the off-diagonal UGDs and virtual gluon—virtual gluon—quarkonium vertex.

We also proposed a way to calculate the soft effects (in the region of small gluon transverse momenta) using the GBW or RS UGDs, which were obtained from the respective color dipole cross sections and a simple (PST) prescription for its off-diagonal extrapolation. In this case, the cross section is only slightly smaller for η_c than for χ_{c0} production. We have also discussed to which extent the absorption effects for $pp \rightarrow pp\eta_c$ are different than those for $pp \rightarrow pp\chi_{c0}$. We find that the absorptive corrections for the η_c are somewhat smaller, which correlates with a very different (t_1, t_2) dependence for the corresponding Born amplitudes. However, there is a rather strong model dependence on the Born amplitude.

It would be desirable to measure the cross section for $pp \rightarrow pp\eta_c$ by identifying η_c , e.g., in the $p\bar{p}$ decay channel as was done in the inclusive case. It could be interesting to estimate the signal-to-background ratio before the real experiment. The $pp \rightarrow ppp\bar{p}$ continuum

was calculated previously by Lebedowicz *et al.* [36], and first experimental evidence was obtained very recently by the STAR Collaboration at the Relativistic Heavy Ion Collider [37]. Also, the $pp \rightarrow ppp\gamma\gamma$ reaction could be considered as an alternative to measure the $pp \rightarrow pp\eta_c$ reaction.

ACKNOWLEDGMENTS

The stay of I.B. in Lund was supported by Polish National Agency for Academic Exchange under Contract No. PPN/IWA/2018/1/00031/U/0001. This study was partially supported by the Polish National Science Center under Grant No. 2018/31/B/ST2/03537 and by the Center for Innovation and Transfer of Natural Sciences and Engineering Knowledge in Rzeszów (Poland). R.P. was partially supported by the Swedish Research Council Grant No. 2016-05996 and by the European Research Council (ERC) under the European Union's Horizon 2020 research and innovation programme (Grant No. 668679).

-
- [1] V. A. Khoze, A. D. Martin, M. G. Ryskin, and W. J. Stirling, *Eur. Phys. J. C* **35**, 211 (2004); L. A. Harland-Lang, V. A. Khoze, M. G. Ryskin, and W. J. Stirling, *Int. J. Mod. Phys. A* **29**, 1430031 (2014).
 - [2] M. G. Albrow, T. D. Coughlin, and J. R. Forshaw, *Prog. Part. Nucl. Phys.* **65**, 149 (2010).
 - [3] R. S. Pasechnik, A. Szczurek, and O. V. Teryaev, *Phys. Rev. D* **78**, 014007 (2008).
 - [4] R. S. Pasechnik, A. Szczurek, and O. V. Teryaev, *Phys. Lett. B* **680**, 62 (2009).
 - [5] R. S. Pasechnik, A. Szczurek, and O. V. Teryaev, *Phys. Rev. D* **81**, 034024 (2010).
 - [6] P. Lebedowicz, O. Nachtmann, and A. Szczurek, *Ann. Phys. (Amsterdam)* **344**, 301 (2014).
 - [7] F. Kopp, M. B. Gay Ducati, and M. V. T. Machado, *Phys. Lett. B* **806**, 135492 (2020).
 - [8] I. Babiarz, R. Pasechnik, W. Schäfer, and A. Szczurek, *J. High Energy Phys.* 02 (2020) 037.
 - [9] I. Babiarz, R. Pasechnik, W. Schäfer, and A. Szczurek, *J. High Energy Phys.* 06 (2020) 101.
 - [10] R. Aaij *et al.* (LHCb Collaboration), *Eur. Phys. J. C* **75**, 311 (2015); **80**, 191 (2020).
 - [11] Tichouk, H. Sun, and X. Luo, *Phys. Rev. D* **101**, 094006 (2020).
 - [12] I. Babiarz, V. P. Goncalves, R. Pasechnik, W. Schäfer, and A. Szczurek, *Phys. Rev. D* **100**, 054018 (2019).
 - [13] A. Szczurek, R. Pasechnik, and O. Teryaev, *Phys. Rev. D* **75**, 054021 (2007).
 - [14] A. Donnachie and P. V. Landshoff, *Phys. Lett. B* **185**, 403 (1987).
 - [15] A. Shuvaev, K. J. Golec-Biernat, A. D. Martin, and M. Ryskin, *Phys. Rev. D* **60**, 014015 (1999).
 - [16] J. R. Cudell, A. Dechambre, O. F. Hernandez, and I. P. Ivanov, *Eur. Phys. J. C* **61**, 369 (2009).
 - [17] K. J. Golec-Biernat and M. Wüsthoff, *Phys. Rev. D* **60**, 114023 (1999).
 - [18] K. Golec-Biernat and S. Sapeta, *J. High Energy Phys.* 03 (2018) 102.
 - [19] A. H. Rezaeian and I. Schmidt, *Phys. Rev. D* **88**, 074016 (2013).
 - [20] E. Iancu, K. Itakura, and S. Munier, *Phys. Lett. B* **590**, 199 (2004).
 - [21] P. Jimenez-Delgado and E. Reya, *Phys. Rev. D* **89**, 074049 (2014).
 - [22] M. Gluck, P. Jimenez-Delgado, E. Reya, and C. Schuck, *Phys. Lett. B* **664**, 133 (2008).
 - [23] M. Gluck, E. Reya, and A. Vogt, *Z. Phys. C* **67**, 433 (1995).
 - [24] J. D. Bjorken, *Phys. Rev. D* **47**, 101 (1993).
 - [25] E. Gotsman, E. Levin, and U. Maor, *Phys. Rev. D* **60**, 094011 (1999).
 - [26] A. B. Kaidalov, V. A. Khoze, A. D. Martin, and M. G. Ryskin, *Eur. Phys. J. C* **21**, 521 (2001).
 - [27] S. Ostapchenko and M. Bleicher, *Eur. Phys. J. C* **78**, 67 (2018).
 - [28] C. Flensburg, G. Gustafson, and L. Lönnblad, *J. High Energy Phys.* 12 (2012) 115.
 - [29] C. O. Rasmussen and T. Sjöstrand, *J. High Energy Phys.* 02 (2016) 142.
 - [30] R. S. Pasechnik and B. Z. Kopeliovich, *Eur. Phys. J. C* **71**, 1827 (2011).

- [31] R. Pasechnik, B. Kopeliovich, and I. Potashnikova, *Phys. Rev. D* **86**, 114039 (2012).
- [32] B. Z. Kopeliovich, R. Pasechnik, and I. K. Potashnikova, *Phys. Rev. D* **98**, 114021 (2018).
- [33] L. Lönnblad and R. Žlebčák, *Eur. Phys. J. C* **76**, 668 (2016).
- [34] I. Babiarez, R. Staszewski, and A. Szczurek, *Phys. Lett. B* **771**, 532 (2017).
- [35] G. Antchev *et al.* (TOTEM Collaboration), *Eur. Phys. J. C* **79**, 103 (2019).
- [36] P. Lebiedowicz, O. Nachtmann, and A. Szczurek, *Phys. Rev. D* **97**, 094027 (2018).
- [37] J. Adam *et al.* (STAR Collaboration), *J. High Energy Phys.* **07** (2020) 178.